Proceedings of the Korean Nuclear Society Spring Meeting
Pohang, Korea, May 1999

A Study on the Non-Heating CHF Experiments Using Drilled Plates

Yong-Hoon Jeong, Won-Pil Baek and Soon Heung Chang

Department of Nuclear Engineering
Korea Advanced Institute of Science and Technology

ABSTRACT

The critical heat flux (CHF) has been studied by many researchers from the discovery of that phenomena, and considerable experiments have been conducted. From the beginning of the critical heat flux (CHF) research, experiments have been conducted using direct heating or in-direct heating methods. However, heating experiment is not easy to perform in some aspects: difficulty of heating method, large electric power source, probable failure of test section, electricity related risk, large cost, etc. In this paper, it is suggested that more convenient and profitable way to study pool boiling CHF phenomena using air bubble generated on the drilled plate and overlaying water. By blowing air through drilled plate in water or other fluid, we can model the real boiling on the plate by air-bubbling on the plate. Through the photographic observation of bubble generation, the similar behavior of air bubble is observed comparing with real steam bubble. And, through measuring void fraction near the plate surface using a conduction probe, macrolayer thickness has been estimated, and the difference between nucleate boiling and CHF has been examined. As a result, through this study, the possibility of non-heating CHF experiment has been examined, and the possible applications of this method have been introduced.

I. INTRODUCTION

The critical heat flux (CHF) is an interesting subject studied by many researchers, and hence considerable experiments have been performed and a large number of papers have been published to date. Especially for pool boiling CHF, as we mentioned, considerable experimental works have been performed and several CHF models have been suggested. However, an exact theory of the CHF has not been obtained, and the experimental work has been limited in scale and complexity of test section. Because electric power has to be supplied to heat the test section, large electric power has to be supplied for large test section, and CHF of the complex structure can not be examined. Due to these reasons, non-heating experimental method is introduced by this study. If non-heating method is possible, we can examine the CHF behavior of more large and complex.

To develop non-heating method, an approach from fundamental CHF mechanism has been

pursued. As mentioned above, although there is no exact theory, macrolayer layer dryout model is considered as a most probable model of CHF occurrence. According that model, CHF is occured when the liquid in the macrolayer is depleted by the vaporization before the liquid ingression, which follows large bubble departure on the heater surface. So, the main parameters of CHF are macrolayer thickness and bubble departure frequency. If we can know these two values, we can calculate the corresponding CHF value. In this study, it is attempted to measure the thickness of macrolayer on the drilled plate through which air is blowing in water pool. As a results, the macrolayer thickness can be measured, and it is coincidence with results of previous researchers.

II. BACKGROUND

Earlier experiments by Gaetner [1] and Katto and Yokota [2] and recent experiments, such as Bhat et al. [3], support the presence of the macrolayer under the vapor bubble on the heater surface. Based on these observations, Haramura and Katto (1985) suggested the macrolayer dryout model. They assume that the CHF occurs when the macrolayer is depleted before the detachment of overlaying vapor bubble or bubbles. That can be expressed like following equation:

$$q_{CHF} = \delta_l \rho_l h_{fg} (1 - A_v / A_w) f \qquad (1)$$

where f is the detachment frequency, δ_l the initial macrolayer thickness, A_w the surface area of heater, and A_v the total bottom area of vapor stems. As shown in Eq. 1, the main parameters which can determine CHF are the initial macrolayer thickness and bubble departure frequency. So, many researchers measre the macrolayer thickness. Gaertner [1] observed macrolayers using an upward-facing 50 mm diameter horizontal disk and discussed the realtion between the macrolayer thickness and the diameter of vapor stems in the macrolayer. After him, considerable measurements have been performed using conduction probe. In most experiments the interface of macrolayer is determined by the position where the void fraction or bubble frequency changes drastically. From the heater wall to the boundary of macrolayer, the void fraction or fluxation frequency is nearly constant. Near the boundary, the void fraction increase drastically and the fluxation frequency is decrease drastically. From these evidences, they determine the macrolayer thickness.

In this paper, void fraction was measured using conduction probe in air-water system, macrolayer thickness was determined, and non-hating method for CHF experiment was suggested. In this experiment, vapor generation on the heater surface was modeled by generation of air bubble using drilled plate instead of direct heating of heater surface.

III. EXPERIMENTS

3.1 Experimental apparatus and procedure

Fig. 1 shows a cross section of the experimental apparatus with a drilled plate. The air-blowing surface is 20 to 50 mm in diameter and made of copper. There are many holes which model active nucleation sites. The pitch of the holes is 1 mm and the diameter of the holes is 0.3 mm.

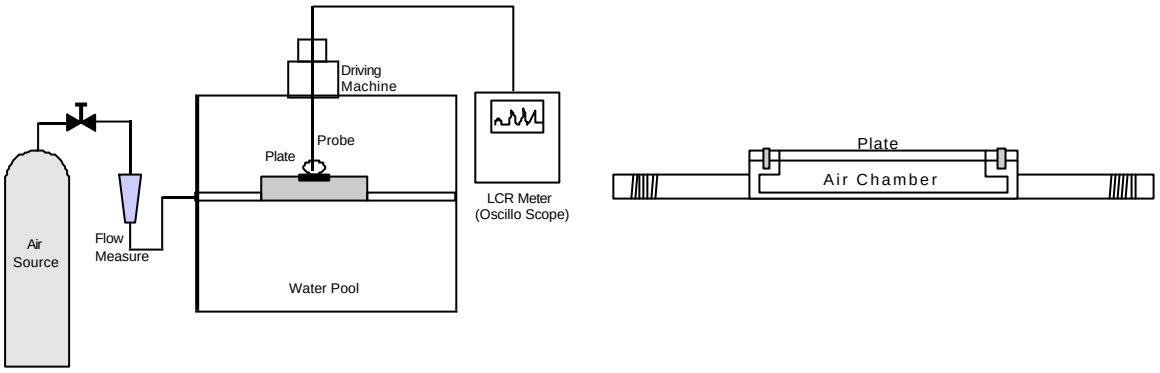

(a) Arrangement of apparatus (b) Cross section of test section

Fig. 1. Experimental apparatus

Wang and Dhir's correlation [5] and Paul and Abdel-Khalik's correlation [6] was used to estimate active nucleation site density. Wang and Dihr correlate their data of active nucleation site density as a function of the wall superheat and contact angle as follows:

$$N = 5\times10^{-27}(1-\cos f)/d_c^6 \tag{2}$$

where the cavity mouth diameter d_c is a function of the local superheating,

$$d_c = \frac{4\sigma T_{sat}}{\rho_g h_{fg}\Delta T} \tag{3}$$

For water under atmospheric pressure, contact angle is about 85° [7], and wall superheat is about 10-20 °C. So, the active nucleation site density is about 60000-4000000 sites/m^2, and is about 250-2000 sites/m. In other words, the pitch between active nucleation site is about 0.5-4 mm. Abdel-Khalik's correlation is equated as follows:

$$N = 1.207\times10^{-3}q + 15.74 \tag{4}$$

Because CHF for flat plate is about 1300 kW/m^2, the active nucleation site density is about 1585 sites/m. In other words, the pitch between active nucleation site is about 0.6 mm. Considering above results, the active nucleation site density is about 1000 sites/m, and the pitch between sites is

about 1mm, which is the same as that of drilled plate.

For the CHF on the flat plate, we assume 1300 kW/m^2 as a CHF. The CHF for flat plate is predicted as 1110 kW/m^2 by Zuber's model [8] for water under atmospheric pressure, and 1260 kW/m^2 by Lienhard and Dhir's model [9]. However, according to experiments, CHF is somewhat larger than two models. So, we assume the CHF like above, and blow air through drilled plate corresponding to that CHF value in this experiment.

To measure void fraction, conduction probe was used. The conduction probe is consisted of two needles with 1 mm of distance between two needles. The resistance or voltage drop across the two needles have been measured by the dynamic signal analyzer (HP 35665A).

3.2 Measurement of void fraction and macrolayer thickness

The void fractions of flat disks have been measured. The disks are 20 to 40 mm in diameter, and have many holes which are 0.3 mm in diameter. The absolute value of the void fraction could not be measured, but the relative distribution could be measured by measuring resistance or voltage drop between tow needles of conduction prob. Actually, the time-averaged resistance is inversely proportional to the void fraction, and the time-averaged voltage is proportional to the void fraction. So, the inverse of resistance and voltage are used as measure of the void fraction.

The void fraction of 20 mm disk is shown in Fig. 2. The air flow of 38.5 scf/min is corresponded to vapor generation rate at CHF. As shown in that figure, the void fraction (time-averaged resistance) is nearly constant and low in the near most region from the wall, and the void fraction is increase with the increase of distance from the wall. The first transition point of the void fraction is about 0.1 mm. And, that point is defined as the macrolayer thickness. However, that value is similar with that of other researchers.

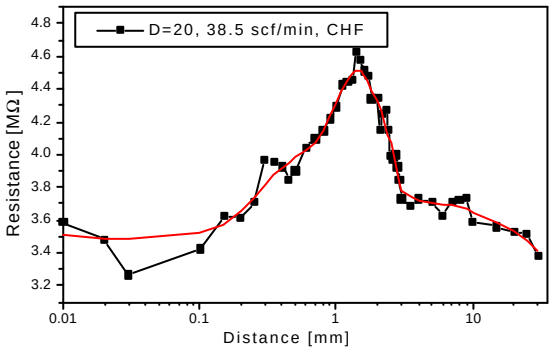

Fig. 2. Void fraction of 20 mm disk at CHF

The void fraction of 25 mm disk is shown in Fig. 3. The air flow of 60 scf/min is corresponded to vapor generation rate at CHF. As shown in that figure, the void fraction (inverse of time-averaged voltage) is also nearly constant and low in the near most region from the wall, and the void fraction is increase with the increase of distance from the wall. The first transition point of the void fraction is also about 0.1 mm. And, that point can be defined as the macrolayer thickness. In the repeated experiments, the distribution of void fraction is nearly same. The absolute value of voltage is somewhat different in these experiments, because of different level of impurities in water. However, the relative distributions coincide with each other.

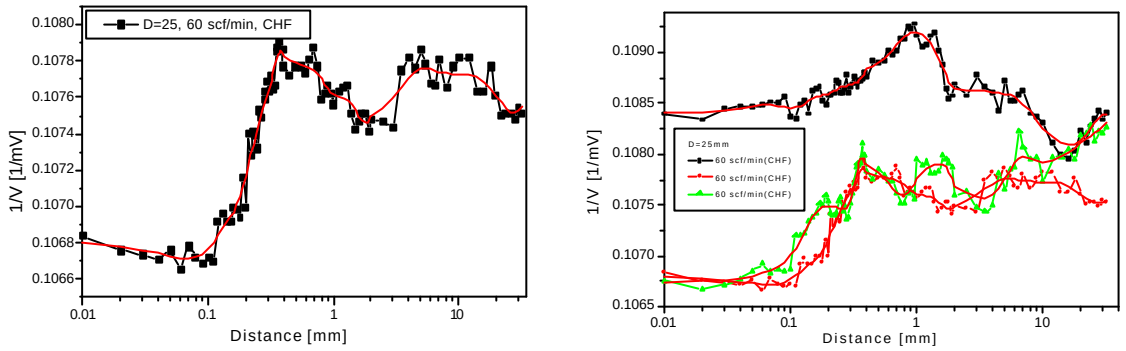

Fig. 3. Void fraction of 25 mm disk at CHF

The void fractions of 30 and 40 mm disk are shown in Fig. 4 and 5. The air flows are corresponded to vapor generation rate at CHF. As shown in that figures, the void fractions (time-averaged resistance or the inverse of time averaged voltage) are also nearly constant and low in the near most region from the wall, and the void fraction is increase with the increase of distance from the wall. The first transition point of the void fraction is also about 0.1 mm. And, that point can be defined as the macrolayer thickness. However, in the region above 1 mm, Fig. 5 shows a different trend comparing with previous results. It may caused by the fluctuation of pool water in that region. In addition, it is clear that the resistance and the inverse of the voltage shows the same results for the void fraction as we expected.

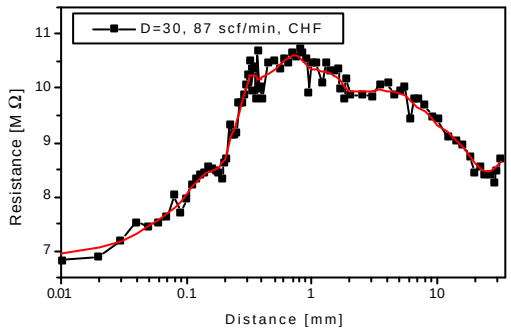

FIg. 4. Void fraction of 30 mm disk at CHF

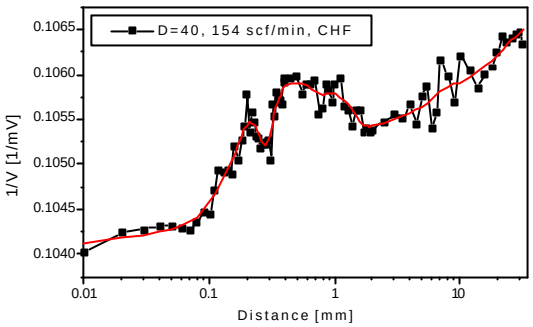

Fig. 5. Void fraction of 40 mm disk at CHF

From above results, it can be drawn that the macrolayer formation on the heater surface can be modeled by air-water system using drilled plate. And, by measuring the resistance or voltage, the distribution of void fraction can be examined and the macrolayer thickness can be estimated from that distribution.

In this study, the difference between nucleate boiling and CHF has been examined at the point of view of void fraction. As shown in Fig. 6 and 7, the void fraction at 2/3 CHF is totally different with that at CHF which is shown in Fig. 3. There is no transition point at which macrolayer thickness can be defined. But, for 5/6 CHF case, the void fraction is similar with that at CHF.

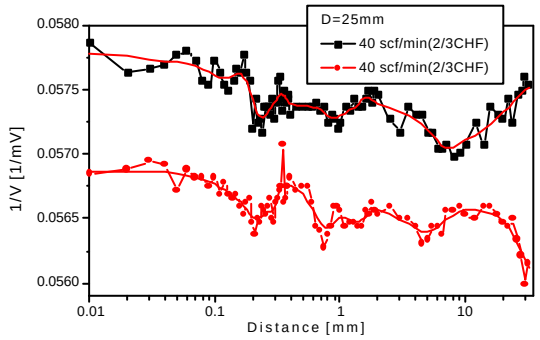

Fig. 6. Void fraction of 25 mm disk at 2/3CHF

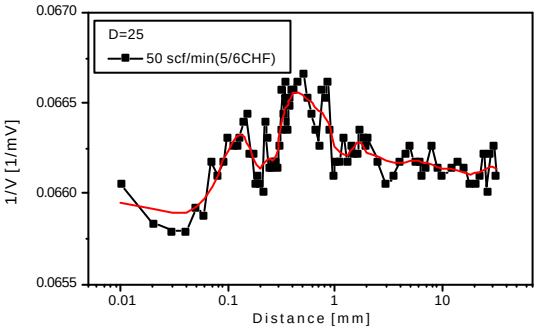

Fig. 7. Void fraction of 25 mm disk at 5/6CHF

Another experiments have been conducted to examine the distribution of void fraction in nucleate boiling region. As shown in Fig. 8 and 9, the void fraction at 70% of CHF is somewhat different with that at 90% of CHF. In Fig. 8, there is no transition point at which macrolayer thickness can be defined. But, for 90%of CHF case, the distribution of void fraction is similar with that at CHF. From these results, it can be drawn that the macrolayer can be stabilized near

CHF. This may be caused by the ingression of overlaying water to air-blowing surface in the case of nucleate boiling. In other words, for lower heat flux (in this study, lower blowing rate), the overlaying water can penetrate into the macrolayer and perturbs that layer because of low velocity of vapor (in this study, air).

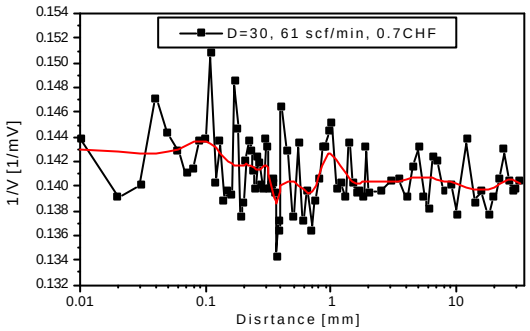

Fig. 8. Void fraction of 25 mm disk at 0.7CHF

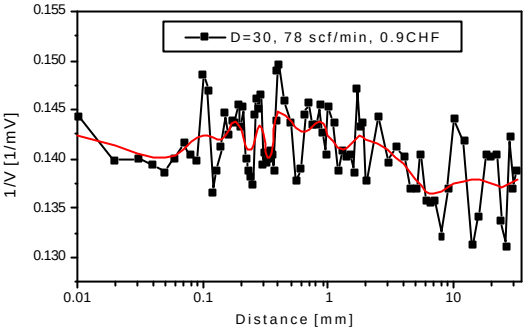

Fig. 9. Void fraction of 25 mm disk at 0.9CHF

IV. CONCLUSION AND RECOMMENDATIONS

A series of non-heating experiments have been conducted to model heating experiment and to estimate the macrolayer thickness. Important findings from this study are summarized as follows:

(a) The void fraction on the air-blowing surface can be estimated using time-averaged resistance or voltage drop across two tips of conduction probe.

(b) From the distribution of void fraction, the macrolyer thickness can be estimated. The first increasing point of the void fraction can be defined as a macrolayer boundary.

(c) From nucleate boiling to CHF, the macrolayer is getting stable. In other words, it is more easier to define the macrolayer boundary at CHF point, than to define it under CHF point.

(d) The suggested non-heating experimental method can be applied to more complex gepmetry where the heating CHF experiment is difficult and expansive.

V. REFERENCES

1. R.F. Gaertner, Photographic study of nucleate boiling on a horizontal surface, ASME J. Heat Transfer, Vol. 87, 17-29, 1965.

2. Y. Katto and Y. Yokoya, Mechanisms of burnout and transition boiling in pool boiling, Trans. JSME, Vol. 37[295], 535-545, 1971.
3. A.M. Bhat, R. Prakash and J.S. Saini, On the mechanism of macrolayer formation in nucleate boiling at high heat flux, Int. J. Heat Mass Transfer, Vol. 26, 735-740, 1986.
4. Y. Haramura and Y. Katto, New hydrodynamic model for critical heat flux (CHF), Trans. JSME, Vol. 49[445], 1919-1927, 1986.
5. C.H. Wang and V.K. Dihr, Effect of surface wettability on active nucleation site density during pool boiling of water on a vertical surface, J. Heat Transfer, Vol. 115, 659-669,1993.
6. D.D. Paul and S.I. Adel-Khalik, A statistical analysis of saturated nucleate boiling along a heated wire, Int. J. Heat Mass Transfer, Vol. 26[4], 509-519, 1983.
7. J.G. Collier and L.R. Thome, Convective boiling and condensation, Clarendon Press, 3rd Edition, p. 142, 1994.
8. N. Zuber, Hydrodynamic aspects of boiling heat transfer, AEC Report AECU-4439, Physics and Mathematics, 1959.
9. J.H. Lienhard, A heat transfer textbook, Prentice-Hall, p. 404, 1981.

NOMENCLATURE

A_v	total bottom area of vapor stems	m^2
A_w	surface area of heater	m^2
d_c	cavity mouth diameter	m
f	detachment frequency	Hz
h_{fg}	heat of vaporization	J/kgK
N	active nucleation density	$sites/m^2 \; or \; sites/m$
T_{sat}	saturation temperature	K
ΔT	wall super heat	K
q_{CHF}	critical heat flux	W/m^2
d_l	initial macrolayer thickness	m
ϕ	contact angle between heater surface and bubble	-
ρ_g	vapor density	kg/m^3
ρ_l	liquid density	kg/m^3
σ	surface tension	kg/m^3